Report no. changed (Mar 2006): SR-215-UU

SACLANTCEN REPORT
serial no.: SR-215

SACLANT UNDERSEA RESEARCH CENTRE

REPORT

Robust broadband matched-field processing: Performance in shallow water by simulation

D.F. Gingras

November 1993

Report no. changed (Mar 2006): SR-215-UU

Page count for SR-215 (excluding Covers and Data Sheet)

Pages	Total
i–vi	6
1–29	29
	35

SACLANT Undersea Research Centre
Viale San Bartolomeo 400
19138 San Bartolomeo (SP), Italy

tel: 0187 540 111
fax: 0187 524 600
telex: 271148 SACENT I

NORTH ATLANTIC TREATY ORGANIZATION

SACLANTCEN SR-215

Robust broadband matched-field processing: Performance in shallow water by simulation

D.F. Gingras

The content of this document pertains to work performed under Project 02 of the SACLANTCEN Programme of Work. The document has been approved for release by The Director, SACLANTCEN.

David L. Bradley
Director

intentionally blank page

SACLANTCEN SR-215

Robust broadband matched-field processing: Performance in shallow water by simulation

D.F. Gingras

Executive Summary: Matched-field processing (the incorporation of acoustic modelling into target localization array processing) has been demonstrated to provide accurate estimates of target depth and range when the environment is well known. When the environment is imprecisely known the performance degrades. In a previous report, SR-201, robust matched-field processing methods were developed. In this report the performance of the robust methods is evaluated and reported for a range-independent shallow-water application.

The performance of the robust methods was compared with that of the nominal processor, that is, the processor based on a single set of environmental parameters thought to be closest to the actual. The simulation results indicate that the robust methods provide significant performance improvements over the nominal processor.

Computer simulation methods were used to perform the evaluation. The matched-field processing performance was evaluated in terms of the peak-to-largest sidelobe ratio. Performance results were computed as a function of uncertainty in water-column sound speed, channel depth and sound speed in the bottom.

This report discusses an improvement to the matched-field processing algorithm which may improve the estimate of a target's depth and range, especially in shallow water. The next step is to evaluate the performance of this algorithm using actual target data.

intentionally blank page

SACLANTCEN SR-215

Robust broadband matched-field processing: Performance in shallow water by simulation

D.F. Gingras

Abstract: An issue of concern for matched-field processing is the strong dependence between performance and precise knowledge about the environmental parameters. Recently a robust matched-field processor based on minimax robust filtering methods was developed. In this report simulation methods are employed to evaluate the performance of the minimax robust method as well as other robust methods for a range-independent shallow-water environment. The performance of the robust methods is compared with that of the nominal processor, that is, the processor based on a single set of environmental parameters thought to be closest to the actual. The matched-field processing performance is evaluated in terms of the peak-to-sidelobe ratio, the simulation results indicate that the robust methods provide significant performance improvements over the nominal processor in the presence of uncertainty in water-column sound-speed, channel depth and sound speed in the bottom.

Keywords: Matched-field processing ○ minimax methods ○ normal-mode modelling.

Contents

1 Introduction

The work of Hinich [1] and Bucker [2], which uses a deterministic full-field acoustic model to accurately predict the properties of the underwater channel, has been applied to array signal processing [3]. This method of array processing is usually referred to as 'matched-field' processing. There has been a number of papers that have dealt with the effect of uncertainty about environmental knowledge on the performance of matched-field processing [4-9]. References [4-8] discuss this problem for shallow-water applications, in general, analyzing the effects of environmental and system parameter uncertainty on processor performance at a single frequency for one or a small number of source locations. Reference [9] provides somewhat more general methods for predicting the effect of environmental uncertainty on detection performance for any specific environment and system. In summary, the major effects of uncertain environmental knowledge on the performance of matched-field processing are: (i) a reduction in the ratio between the peak amplitude at the source location to the amplitude of the highest sidelobe, and (ii) error in the location of the source peak in range and depth. It can be concluded that for most applications the performance of matched-field processing is very sensitive to uncertainty about environmental knowledge.

It is apparent that acoustic model-based array signal processing methods that are robust or tolerant of uncertainty in environmental knowledge are required. In most design problems, including array processing, there is a performance measure $M(h,q)$ which is to be minimized to design a filter h, where $h \in H$ and H is a space of possible designs, under an operating condition q, where $q \in Q$ and Q is a possible set of operating points or models, see Ref. [10]. The traditional design approach is to select a particular model $q_o \in Q$ and determine h_o such that

$$M(h_o, q_0) = \min_{h \in H} M(h, q_o).$$

The usual array processor is of this form where h is a matched filter based on a single representation of the environment q_o. This design approach makes no allowance for tolerance to uncertainty in the model point q_o. If, in fact, it is known that knowledge about q_o is uncertain and that q_o actually may fall in some neighborhood P then it would be important to know the worst case performance of h over P, i.e., the quantity

$$\max_{q \in P} M(h, q).$$

The minimax criterion is based on the minimization of this worst case performance,

The objective of this report is to provide an evaluation of the performance of robust matched-field processing methods for a canonical shallow-water environment. In assessing the performance of robust methods there are two factors of major interest: (1) the degree to which the performance of the nominal processor is degraded relative to that of the robust processor, and (2) the degree to which the nominal processor outperforms the robust processor when the nominal environment is actually present. Also, since one can rarely place an absolute maximum value on the degree of environmental uncertainty, it is of interest to assess the behavior of the robust processor when the degree of uncertainty differs from that assumed in the robust design. This can provide useful information for deciding which robust processor achieves the best trade-off of worst case performance versus behavior close to the nominal processor. The nominal processor is the non-robust processor which is based on a single set of environmental parameters which are thought to be closest to the actual set of environmental parameters.

Two canonical shallow-water environments, one winter and one summer, are considered. The performance of the nominal and robust processors is evaluated in terms of 'peak-to-sidelobe' ratio as a function of the degree of uncertainty about environmental knowledge and as a function of the expected degree of uncertainty used in the design of the robust processor. In Sect. 2 matched-field processing in terms of the channel transfer function is discussed. In Sect. 3 robust processing is discussed in terms of the matched-field processing problem. In Sect. 4 the performance of the processors is evaluated for shallow-water environments as a function of uncertainty about the water-column sound-speed, the channel depth and the sound speed in the bottom. Sect. 5 provides a discussion of the results.

Throughout this report vectors are denoted by boldface lower case letters, matrices are denoted by upper case letters and $\mathbf{u}^*$ indicates conjugate transpose of the vector $\mathbf{u}$.

2

Acoustic model-based processing

We assume throughout that we are working in a horizontally stratified acoustic waveguide or channel which is characterized by a depth varying sound speed and certain boundary conditions. A cylindrical coordinate system $\{r, \rho, z\}$ is used with the depth axis, the z-axis, passing through the receivers. The field is assumed to be independent of azimuthal angle, ρ. Furthermore, we assume that the propagation of acoustic signals through the channel can be described by the linear, inhomogeneous, scalar wave equation. Since the wave equation for small-amplitude acoustic signals is linear we can represent the channel as a linear time-invariant space-variant filter. The channel impulse response function, $h_{\mathbf{v_j}}(\boldsymbol{\beta}, \boldsymbol{\theta}; t)$, is a linear time-invariant space-variant function of the receiver location $\mathbf{v}_j$, the source location $\boldsymbol{\beta} = (r, z)$, and a vector of channel parameters $\boldsymbol{\theta}$ which contains the environmental properties for the specific acoustic channel. Since most numerical solutions of the wave equation are developed under the assumption that the source is a point source radiating at a single frequency we use the channel transfer function, Fourier transform of the impulse response function. We define the channel transfer function over a set of discrete frequencies, $\omega = \omega_n \; n = 1, \ldots, N$. The environmental parameters usually consist of at least the sound speed vs depth in the water column, the thickness, density, attenuation and sound speed vs depth for the sediment and bottom density, attenuation and sound speed.

Since the receivers are located on the depth axis at the origin of the coordinate system, let the subscript j denote the receiver depth coordinate and represent the channel impulse response function by $h_j(\boldsymbol{\beta}, \boldsymbol{\tau}; t)$. Assume that there is a single broadband source plus additive noise, the observations at the jth sensor are modeled as

$$y_j(t) = u(t) * h_j(\boldsymbol{\beta}, \boldsymbol{\theta}; t) + n_j(t) \tag{1}$$

for $t = 0, 1, \ldots, T-1$ and $1 \leq j \leq L$, where: $\boldsymbol{\beta}$ is the vector indicating the location of a broadband source, j is the index for vector $\mathbf{v}_j$ which denotes the location of the jth sensor, $u(t)$ is a random process radiated by the source, $h_j(\boldsymbol{\beta}, \boldsymbol{\theta}; t)$ is the channel impulse response function for the channel between the source at $\boldsymbol{\beta}$ and the sensor at $\mathbf{v}_j$, $\boldsymbol{\theta}$ is the vector containing knowledge about the environment, $n_j(t)$ is additive noise at the jth sensor, and $*$ denotes convolution.

The source process $u(t)$ is a broadband zero-mean stationary Gaussian process, uncorrelated with the additive noises with spectral density $\phi_u(\omega)$. While $u(t)$ is not strictly defined as a bandlimited process we assume that a majority of its power is in a finite band of width B Hz. The additive noises $\{n_j(t)\}$ are broadband zero-mean correlated stationary Gaussian processes with cross spectral density matrix $\mathbf{Q}(\omega)$.

The sensor outputs are observed for a common time interval of T seconds, which is long compared to the random process correlation times, long compared to the propagation time of the source process across the array and greater than the duration of the channel impulse response. Since the observation interval is finite we represent the observations using a finite Fourier transform representation. The normalized Fourier coefficients $\{y_j(\omega), \omega \in B\}$ are given by

$$y_j(\omega) = (1/\sqrt{T}) \sum_{t=0}^{T-1} y_j(t) \exp(-i\omega t). \tag{2}$$

We assume that the impulse response function is such that

$$\sum_{t=-\infty}^{\infty} (1 + |t|)|h(\boldsymbol{\beta}, \boldsymbol{\theta}; t)| < \infty \tag{3}$$

then the Fourier transform representation for the impulse response or transfer function is given by

$$h(\boldsymbol{\beta}, \boldsymbol{\theta}; \omega) = \sum_{t=-\infty}^{\infty} h(\boldsymbol{\beta}, \boldsymbol{\theta}; t) \exp(-i\omega t). \tag{4}$$

Define the channel transfer function vector $\mathbf{h}(\boldsymbol{\beta}, \boldsymbol{\theta}; \omega_n)$ to be a unit norm vector

$$\mathbf{h}(\boldsymbol{\beta}, \boldsymbol{\theta}; \omega_n) = \frac{(h_1(\boldsymbol{\beta}, \boldsymbol{\theta}; \omega_n), h_2(\boldsymbol{\beta}, \boldsymbol{\theta}; \omega_n), \ldots, h_{\mathrm{L}}(\boldsymbol{\beta}, \boldsymbol{\theta}; \omega_n))^{\mathrm{T}}}{|(h_1(\boldsymbol{\beta}, \boldsymbol{\theta}; \omega_n), h_2(\boldsymbol{\beta}, \boldsymbol{\theta}; \omega_n), \ldots, h_{\mathrm{L}}(\boldsymbol{\beta}, \boldsymbol{\theta}; \omega_n))|}. \tag{5}$$

Under the assumption that the observation interval T is long, compared to the correlation lengths of the signal and noise processes, we make the usual assumption that the Fourier coefficients are uncorrelated across frequency. Furthermore we assume that the noise processes are spatially uncorrelated with the same spectrum, let $\mathbf{Q}(\omega_n) = \phi_n(\omega_n)\underline{\mathrm{I}}$, then a derivation of the likelihood ratio detector, see Ref. [13], yields the familiar 'Bartlett' likelihood ratio or matched filter processor, i.e.,

$$\Lambda(\boldsymbol{\beta}) = \sum_{n=1}^{N} |\gamma(\omega_n)\mathbf{h}^*(\boldsymbol{\beta}, \boldsymbol{\theta}; \omega_n)\mathbf{y}(\omega_n)|^2 \tag{6}$$

where

$$|\gamma(\omega_n)|^2 = \frac{\phi_u(\omega_n)/\phi_n(\omega_n)}{\phi_u(\omega_n) + \phi_n(\omega_n)}. \tag{7}$$

The broadband frequency weighting term, $|\gamma(\omega_n)|^2$, of Eq. (7), was developed using the likelihood ratio criteria. Other criteria have been used to develop broadband frequency weighting schemes, alternative schemes include the Eckart filter where

$$|\gamma(\omega_n)|^2 = \frac{\phi_u(\omega_n)}{\phi_n(\omega_n)^2} \tag{8}$$

and the Wiener filter where

$$|\gamma(\omega_n)|^2 = \frac{\phi_u(\omega_n)}{\phi_u(\omega_n) + \phi_n(\omega_n)}. \tag{9}$$

Since the observations $\mathbf{y}(\omega)$ are random the detection statistic $\Lambda(\boldsymbol{\beta})$ will be random. In general it will be of interest to consider the mean of the detection statistic, thus define the covariance matrix of the observation vectors to be $\mathbf{R}(\omega) \equiv E[\mathbf{y}(\omega)\mathbf{y}^*(\omega)]$. The mean of the detection statistic is given by

$$E[\Lambda(\boldsymbol{\beta})] \equiv \sum_{n=1}^{N} |\gamma(\omega_n)|^2 \mathbf{h}^*(\boldsymbol{\beta}, \boldsymbol{\theta}; \omega_n) \mathbf{R}(\omega_n) \mathbf{h}(\boldsymbol{\beta}, \boldsymbol{\theta}; \omega_n). \tag{10}$$

We see from Eq.(10) that the channel transfer function vector $\mathbf{h}(\boldsymbol{\beta}, \boldsymbol{\theta}; \omega_n)$ between an assumed source position $\boldsymbol{\beta}$ and the sensor locations $\{\mathbf{v}_j\} j = 1, \ldots, L$ provides the detailed information about the acoustic channel which is integral to matched-field processing. We remark that our ability to accurately predict the channel transfer function, which in turn is strongly dependent on the accuracy of the environmental knowledge, is a major factor affecting the performance of matched-field processors. Equation (10) represents a formulation for a broadband 'Bartlett' matched-field processor in terms of the channel transfer function.

3

Robust matched-field processing

In the previous section a 'Bartlett' matched-field matched filter processor, which was derived using a likelihood ratio formulation, was presented. The development of this processor was carried out under the assumption that knowledge about the channel parameter vector $\boldsymbol{\theta}$ was exact. In most situations the environmental parameters are not known exactly but the degree of uncertainty may be known. In this case a desirable solution to the environmental uncertainty problem is the development of a processor that is robust to the uncertainty. As seen by the likelihood ratio detector formulation leading up to the matched filter processor of Eq. (10) the signal replica term of the matched filter is given by $\gamma(\omega)\mathbf{h}(\boldsymbol{\beta}, \boldsymbol{\theta}; \omega)$. Since it is assumed that the source signal and noise spectra are known, i.e., $\gamma(\omega)$ is exactly known, only the channel transfer function vector $\mathbf{h}$ will be modified to form the robust matched filter.

The uncertainty about environmental parameters will produce an equivalent uncertainty about the channel transfer function $\mathbf{h}(\omega)$, see Ref. [11]. In this situation, even though $\mathbf{h}(\omega)$ is not known exactly, the information about the degree of uncertainty about the environmental parameters can be used to predict a class of channel characteristics, denote it by H, that contains $\mathbf{h}(\omega)$. In this case a matched filter must be designed for the set H of possible channel characteristics. In general, no single filter will be optimum for every member of the uncertainty class. It is desirable to design a robust filter, i.e., one whose performance is as close as possible to the optimum regardless of which member of the uncertainty set is present. A well-established approach for this robust filtering problem, developed in the communications systems literature, is the minimax method [10], [12]. The minimax design goal is to optimize the worst case performance over the uncertainty class H.

Figure 1 *Uncertain linear channel $h(\omega)$ and linear filter $g(\omega)$.*

The system under consideration is illustrated by Fig. 1. Let $h(\omega)$ denote any one of the elements of the channel vector $\mathbf{h}(\omega)$. The input process $u(t)$ is transformed by the imprecisely known channel, represented by $h \in H$, the output of the channel is transformed by the filter $g \in G$, where G denotes the class of possible solutions for g.

The robust design goal is, for $h \in H$, determine the filter $g \in G$ which minimizes the mean square error (MSE) between the input $u(t)$ and the output $\hat{u}(t)$. It is straight forward to show that the MSE, $e(h, g)$, between the system output and input is given by

$$e(h, g) = \sum_{n=1}^{N} |1 - h(\omega_n)g(\omega_n)|^2 \phi_u(\omega_n). \tag{11}$$

A filter which guarantees an upper bound on the mean square error $e(h, g)$ of Eq. (11) over the class of channel characteristics H is desired. A filter with this property can be considered a robust filter for the class H in the sense that a certain level of performance can be guaranteed by using such a filter. It is desirable to have the best such filter, that is, to find a minimax filter g_{M} which satisfies

$$\min_{g \in G} \max_{h \in H} e(h, g) = \max_{h \in H} e(h, g_M). \tag{12}$$

Thus, $g_{\mathrm{M}}(\omega_n)$ $n = 1, \ldots, N$ will be the transfer function of a minimax filter which optimizes worst case performance for the class H of expected channel characteristics.

3.1. ROBUST TRANSFER FUNCTION METHODS

We assume that the channel transfer function modulus is a measurable function and that it is bounded by the two known measurable functions $h_{\mathrm{L}}(\omega_n)$ and $h_{\mathrm{U}}(\omega_n)$ such that

$$0 < h_{\mathrm{L}}(\omega_n) \leq |h(\omega_n)| \leq h_{\mathrm{U}}(\omega_n) < \infty. \tag{13}$$

Let the phase characteristic of the channel, $\arg\{h(\omega_n)\}$, be a measurable function denoted by $\psi_h(\omega_n)$. Assume that, for each ω_n, there is a known closed subset $\Omega(\omega_n)$ of $(-\pi, \pi]$ which contains the value of $\psi_h(\omega_n)$. Thus $[h_{\mathrm{L}}(\omega_n), h_{\mathrm{U}}(\omega_n)]$ and $\Omega(\omega_n)$ define the class H of allowable channel characteristics.

The minimax solution of Eq. (12), $g_{\mathrm{M}}(\omega_n)$, as derived in Ref. [12] and applied to the matched-field problem in Ref. [13] yields a minimax channel transfer function, $h_{\mathrm{minmax}}(\omega_n)$, defined in terms of its modulus and phase as

$$|h_{\mathrm{minmax}}(\omega_n)| = \begin{cases} 0, & \text{if } \cos[\alpha(\omega_n)] \geq 0; \\ -\cos[\alpha(\omega_n)][h_{\mathrm{L}}(\omega_n) + h_{\mathrm{U}}(\omega_n)]/2, & \text{if } \cos[\alpha(\omega_n)] < 0 \end{cases} \tag{14}$$

and

$$\arg\{h_{\mathrm{minmax}}(\omega_n)\} = \gamma_{\mathrm{mid}}(\omega_n), \tag{15}$$

where the angle $\alpha(\omega_n)$, which is one-half of the complement of the phase uncertainty, and the angle $\gamma(\omega_n)$, which is the midpoint of the set $\Omega(\omega_n)$, are defined by Fig. 2.

Note, if the angular span of the subset defining the phase uncertainty $\Omega(\omega_n)$ is greater than π it follows that $0 \leq \alpha(\omega_n) \leq \pi/2$ and $\cos[\alpha(\omega_n)]$ is nonnegative. In

i.e., determine the filter h which minimizes the worst case performance

$$\min_{h \in H} \max_{q \in P} M(h, q).$$

Thus a procedure for designing a robust solution h_R is given by the solution of

$$\max_{q \in P} M(h_R, q) = \min_{h \in H} \max_{q \in P} M(h, q).$$

It is reasonable to assume that the acoustic channel can be modeled as a linear time-invariant space variant filter. Thus, the matched-field processor can be formulated in terms of the time-invariant space-variant filter between all potential source locations in the channel and all receiver locations, see Ref. [11]. As a result of formulating the matched-field processor in terms of the channel filters it is straight forward to apply minimax filtering methods, see Refs. [10] and [12]. A minimax robust matched-field processing method which incorporates knowledge about the environmental parameter uncertainty into the processor design has been developed [13]. An alternative approach, the 'optimum uncertain field processor,' is developed in Ref. [14]. The optimum uncertain field processor allows for inclusion of knowledge about environmental uncertainty by assigning *a priori* probability distributions to the unknown source locations and environmental parameters and then approximating the maximum *a posteriori* probability distribution of the source location, given the observed data.

As discussed in many papers on plane wave and matched-field array processing there are two primary processing methods employed: (1) the linear or 'Bartlett' processor which does not adapt to the signal-plus-noise field and (2) the so-called 'maximum likelihood' or more appropriately the 'minimum variance' processor which does adapt to the signal-plus-noise field. In both Refs. [13] and [14] an environmentally tolerant linear or non-adaptive processor is the resulting processor formulation.

Two papers which provide tolerant minimum variance matched-field processing methods have appeared, see Refs. [15] and [16]. In Ref. [15] a multiple constraint approach is used to provide tolerance to uncertain environmental knowledge. This approach does not take into account *a priori* knowledge about the expected degree of environmental uncertainty. In Ref. [16] multiple linear constraints, derived from predicted pressure fields for a set of perturbed sound speed profiles, are used in the minimum variance processor. This resulting minimum variance processor couples knowledge about the sound- speed uncertainty into the design of the processor and simulation results indicate improvements in performance in deep water. The minimum variance matched-field methods were not considered in this performance evaluation because the performance of these methods is highly dependent on the assumed spatial distribution of the signal-plus-noise field. It was decided that it was more important to emphasize the robust processor performance as a function of the degree of environmental uncertainty without the additional complication of an assumed spatially dependent noise field.

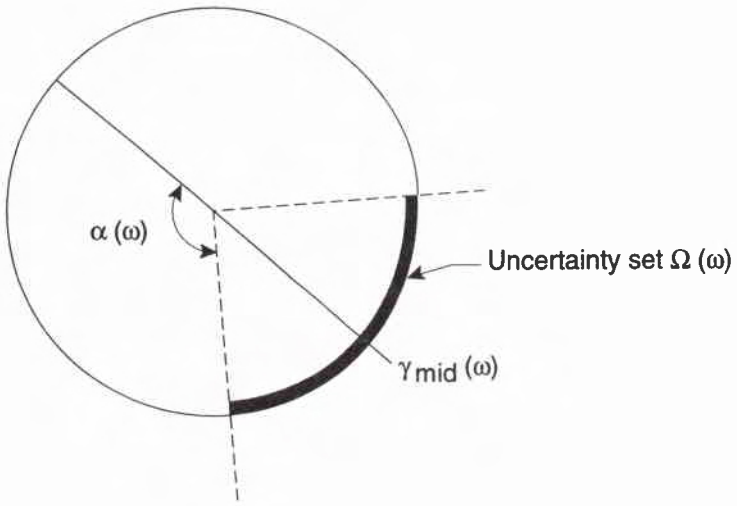

Figure 2 *Uncertainty set $\Omega(\omega)$ and the angles $\alpha(\omega)$ and $\gamma_{\text{mid}}(\omega)$.*

this case the amplitude characteristic of the minimax robust solution is zero, see Eq. (14). When the span of $\Omega(\omega_n)$ is less than π the amplitude characteristic is the midpoint of the amplitude interval times the scale factor $\cos[\alpha(\omega_n)]$. When the phase uncertainty is small, $\alpha(\omega_n)$ approximates π, the scale factor has little or no effect and in this case the amplitude characteristic is essentially $[h_{\text{L}}(\omega_n)+h_{\text{U}}(\omega_n)]/2$. Thus, when the phase and amplitude uncertainty are small the channel characteristic is essentially that of a nominal (exactly known) channel.

It was shown in Ref. [11] that relatively small perturbations of an environmental parameter can cause relatively large variations of the phase of the channel transfer function. That is, at some frequency ω_n for some sensor and source location, the difference between a nominal transfer function phase and a perturbed transfer function phase may be a significant portion of one phase cycle or the uncertainty set $\Omega(\omega_n)$ may be greater than π. As seen above, in this case, the minimax robust processor sets the amplitude characteristic of the minimax robust filter to zero. For the matched-field processing application, in some situations, this solution may too severe. In view of this situation an 'ad hoc' processor, based on the above minimax robust processor, was defined in Ref. [13] and referred to as the midpoint processor $h_{\text{midpt}}(\omega_n)$. This robust processor eliminates the amplitude scale factor $\cos[\alpha(\omega_n)]$ and is defined as follows:

$$|h_{\text{midpt}}(\omega_n)| = [h_{\text{L}}(\omega_n) + h_{\text{U}}(\omega_n)]/2 \tag{16}$$

and

$$\arg\{h_{\text{midpt}}(\omega_n)\} = \gamma_{\text{mid}}(\omega_n). \tag{17}$$

The mean robust method follows when one assumes that the probability distribution of the environmental parameters used in the optimum uncertain field processor of

Ref. [14] is a uniform distribution with the same bounds as used in the minimax solution. In our application the mean robust processor h_{mean} is computed as the mean of the complex transfer functions evaluated at the bounds of the uncertainty class H.

3.2. ROBUST MATCHED-FIELD MATCHED FILTERS

As discussed in Sect. 2 the matched-field matched filter processor based on perfect environmental knowledge is given by Eq. (10) and repeated below, i.e.,

$$E[\Lambda(\boldsymbol{\beta})] \equiv \sum_{n=1}^{N} |\gamma(\omega_n)|^2 \mathbf{h}^*(\boldsymbol{\beta}, \boldsymbol{\theta}; \omega_n) \mathbf{R}(\omega_n) \mathbf{h}(\boldsymbol{\beta}, \boldsymbol{\theta}; \omega_n). \tag{18}$$

The channel transfer function vector $\mathbf{h}(\boldsymbol{\beta}, \boldsymbol{\theta}; \omega_n)$, see Eq. (5), must be evaluated at each sensor location $\underline{\mathrm{v}}_j$; $j = 1, 2, \ldots, L$ for all potential source locations, $\boldsymbol{\beta}$, on the range/depth plane for one environmental parameter vector $\boldsymbol{\theta}$. The implementation of the robust matched-field matched filters is accomplished by substituting the robust transfer function vector, i.e., $\mathbf{h}_{\text{minmax}}$, $\mathbf{h}_{\text{midpt}}$, or $\mathbf{h}_{\text{mean}}$ into Eq. (18) in place of $\mathbf{h}$.

The calculation of the robust transfer function vectors for the robust matched-field processors is as follows. Given that it is known that some environmental parameter θ from the vector $\boldsymbol{\theta}$ is contained in some uncertainty set, call it Q, then a design neighborhood, a subset of Q, is selected. Let the design neighborhood subset be defined by θ_{a} and θ_{b}, then for all possible transfer 'paths' between each sensor and each potential source location on the range/depth plane the transfer function is calculated for both environments, i.e. for θ_{a} and θ_{b}. For all possible 'paths' the bounds on the transfer function modulus, i.e. $h_{\text{L}}(\omega_n)$ and $h_{\text{U}}(\omega_n)$ of Eq. (13), the phase subset $\Omega(\omega_n)$ and the midpoint angle $\gamma_{\text{mid}}(\omega_n)$ are calculated for each frequency ω_n. From these bounds the minimax transfer function vector $\mathbf{h}_{\text{minmax}}(\boldsymbol{\beta}, \boldsymbol{\theta}_{\text{a}}, \boldsymbol{\theta}_{\text{b}}; \omega_n)$ can be evaluated using the method as defined by Eqs. (14) and (15). The midpoint transfer function vectors, $\mathbf{h}_{\text{midpt}}$, can be evaluated similarly using Eqs. (16) and (17). The robust transfer function vectors for the mean processor, $\mathbf{h}_{\text{mean}}$, are computed as the sample mean of the complex transfer functions evaluated at the bounds defined by the design neighborhood for all possible 'paths'.

4

Performance in shallow water

The objective of this section is to present, via simulation, an evaluation of the performance of robust matched-field processing methods and to compare their performance with that of the conventional or nominal matched-field processor. In assessing the performance of robust methods there are two factors of major interest: (1) the degree to which the performance of the nominal processor is degraded relative to that of the robust processor in the presence of uncertainty, and (2) the degree to which the nominal processor outperforms the robust processor when the nominal environment is actually present. In both cases the performance will also be a function of the 'design neighborhood' or subset of the uncertainty space that has been used for the design of the robust processor. The nominal processor is the non-robust processor based on a single set of environmental parameters thought to be closest to the actual environmental parameters.

Two canonical shallow-water environments, one winter and one summer, are considered, see Fig. 3. The winter environment, Fig. 3a, is the same as that used in Ref. [7], a slightly upward refracting sound speed profile, no sediment layer, medium to hard bottom and no shear. Figure 3b illustrates the canonical summer environment, an isovelocity layer down to 20 m, a thermocline from 20 m to 40 m, below 40 m the profile is identical to the winter profile. A center frequency of 250 Hz is used throughout the simulation, at this frequency the channel supports 14 modes.

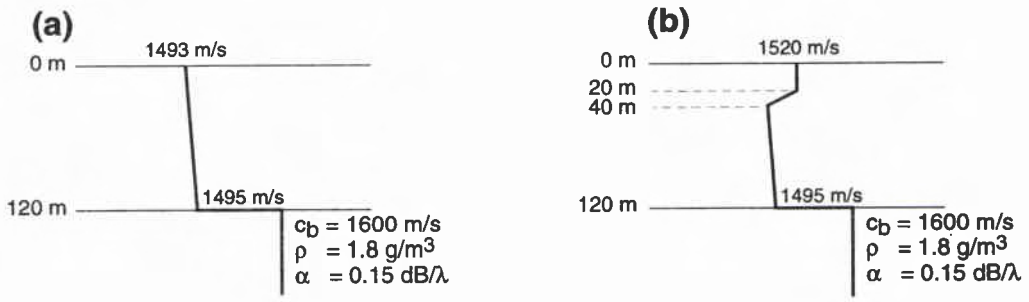

Figure 3 *Canonical shallow-water environments, (a) Winter profile, (b) Summer profile.*

Many papers addressing the performance of non-robust matched-field processing have appeared, see for example Refs. [4-9] and references therein. In almost all cases the measure of performance used to evaluate matched-field processing performance

is the sidelobe structure and its relation in amplitude to the source peak. In this report the performance of the nominal and robust processors is evaluated in terms of the 'peak-to-sidelobe' ratio as a function of the degree of uncertainty about environmental knowledge and as a function of the subset defining the design neighborhood. The 'peak-to-sidelobe' ratio is defined as the difference in dB between the power at the source location to that of the highest sidelobe on the range/depth surface. The peak-to-sidelobe ratio for the highest sidelobe is a good performance measure for matched-field processing because if is there is not a reasonable difference in amplitude between the source peak and the highest sidelobe then in the presence of noise there will be a high probability that the sidelobe plus noise will be greater than the source peak amplitude, resulting in an incorrect source localization.

The performance analysis was conducted via computer simulation, all acoustic model calculations were performed using the SACLANT Centre Normal-mode Acoustic Propagation (SNAP) model [17]. Unfortunately, it is not possible to evaluate the performance of matched-field processing independent of system parameters. In the conduct of these simulations, certain 'system' parameters were selected and kept constant. The selection of these system parameters was somewhat arbitrary and, of course, the performance results presented herein are a function of these parameters. It must be kept in mind that if other system parameters are selected the performance of the methods may vary. The range/depth plane consisted of 1–30 km in range and 2–100 m in depth. The resolution used was 1 km in range and 2 m in depth. The frequency resolution used in the Fourier decomposition was 1.46 Hz across a band from 240 to 260 Hz. The vertical array contained 32 sensors spaced at 3 m with the top sensor at 10 m depth. The broadband signal used was an exponentially damped sinusoid pulse with center frequency of 250 Hz and bandwidth greater than the analysis band, there was no noise added to the signal.

As discussed in Sect. 3, three formulations of robust matched-field processors will be considered; i.e., minimax, defined by Eqs. (14) and (15), midpoint, defined by Eqs. (16) and (17), and the mean, which is formed as the sample mean of the complex transfer functions. In all cases the robust processor is designed over a 'design neighborhood', the notation used to define this neighborhood is minimax(a,b) where a and b are the subset bounds defined in terms of deviations from the nominal value of the environmental parameter.

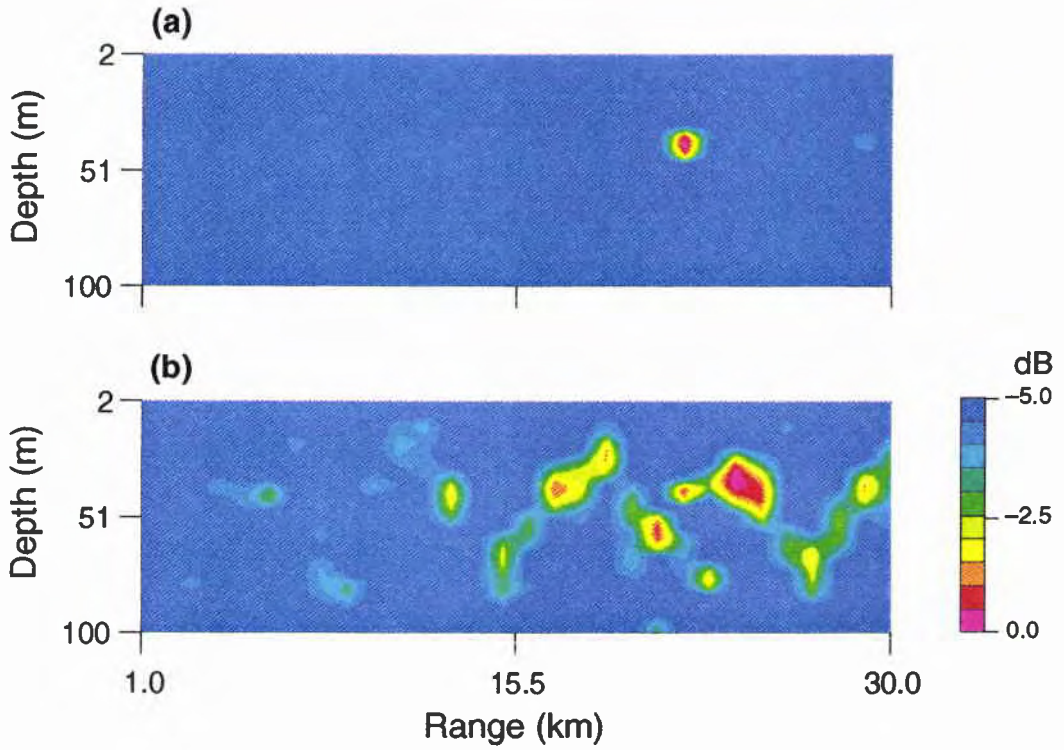

Figure 4 *Matched-field ambiguity surfaces using winter profile for a source at 40 m depth and 22 km range, (a) nominal environment with no uncertainty, (b) with −1 m/s sound-speed uncertainty in the water column.*

4.1. SOUND-SPEED UNCERTAINTY IN THE WATER COLUMN: WINTER PROFILE

In this subsection we present the performance results obtained using the robust and nominal matched-field processors in the presence of sound-speed uncertainty for the canonical winter environment. The sound-speed uncertainty was generated by perturbing the surface value from the nominal value of 1493 m/s to 1492 m/s in steps of 0.2 m/s. This sound-speed perturbation affects both the surface value and the slope of the profile and thus represents a significant degree of sound-speed uncertainty.

Figure 4 illustrates a typical range/depth matched-field ambiguity surface computed using the system parameters defined above for a source at a depth of 40 m and at a range of 22 km using the winter profile. Figure 4a illustrates the case where there is perfect knowledge about the environmental parameters, there are almost no sidelobes within 5 dB of the peak value, only one sidelobe with a peak-to-sidelobe ratio of about 4 dB. Figure 4b illustrates the uncertain environment case where the processor used the nominal environment but the signal was generated using an environment with the sound speed surface value perturbed by −1 m/s with respect to the nominal value. It can be seen from Fig. 4b that the result of this uncertainty is serious. The source peak is not at the correct location and the sidelobe level has increased

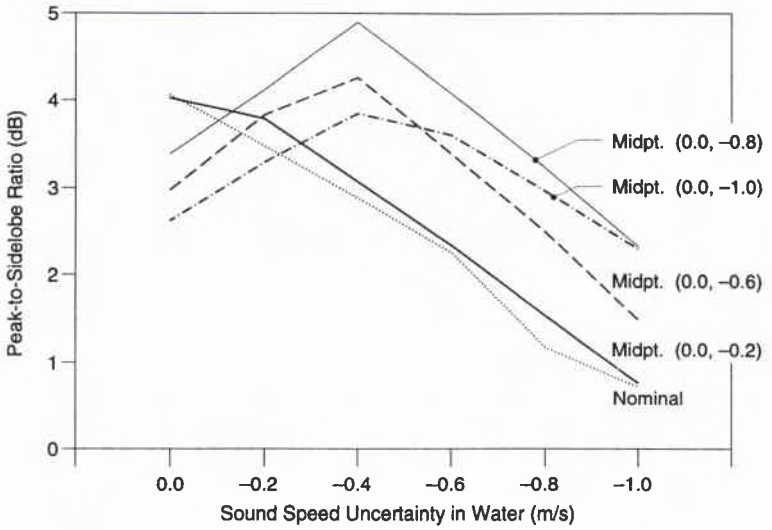

Figure 5 *Peak-to-sidelobe ratio as a function of sound-speed uncertainty in the water column for the 'midpoint' robust processor using the winter profile. Results are shown for the midpoint processor designed using five different uncertainty neighborhoods and for the nominal processor for a source at 40 m depth and 22 km range.*

significantly, the highest sidelobe has a peak-to-sidelobe ratio of only 0.72 dB. Figure 4 provides an indication of the degree of performance degradation which may be experienced in a shallow-water channel with a relatively small uncertainty about the sound speed profile.

Figure 5 illustrates an overview of performance, peak-to-sidelobe ratio, for both the nominal processor and the robust processor as a function of sound speed uncertainty. It is seen that the peak-to-sidelobe ratio for the nominal processor decreases almost monotonically from 4 dB to 0.7 dB as the uncertainty varies from 0 to -1 m/s. The other curves illustrate the performance of the midpoint robust processor for various design neighborhoods. All but one design neighborhood provides a significant improvement in peak-to-sidelobe ratio when there is uncertainty in sound speed greater than about -0.15 m/s. The design neighborhood $(0.0,-0.8)$ provides the greatest improvement in performance. At the maximum uncertainty, -1 m/s, the midpoint $(0.0,-0.8)$ processor provides a 2.3 dB peak-to-sidelobe ratio whereas the nominal processor provides only a 0.7 dB peak-to-sidelobe ratio. Over the entire range of sound-speed uncertainty the midpoint $(0.0,-0.8)$ processor provides a range/depth ambiguity surface with the peak at the correct source location.

It is of interest to note the effect that the design neighborhood has on performance. For any application the selection of the design neighborhood will be important and will greatly affect overall performance. In general, it is desirable to select the design neighborhood so that the performance of the robust processor is close to that of the nominal processor when there is no uncertainty and is better than the nominal when

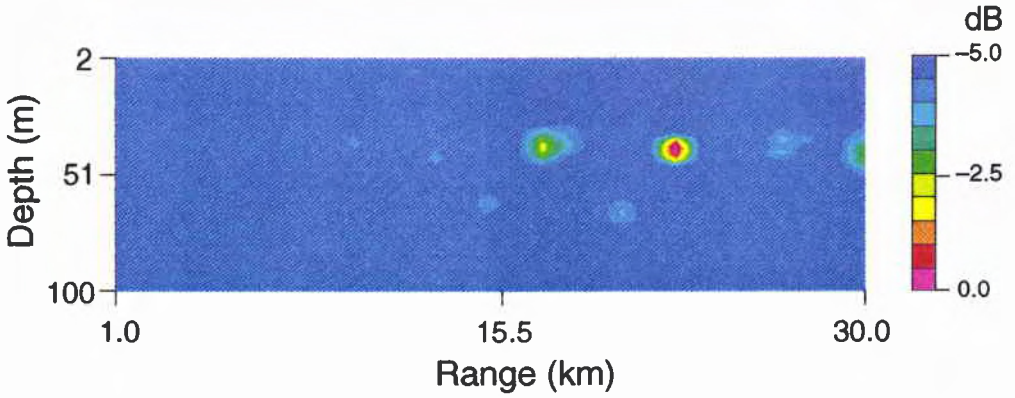

Figure 6 *Matched-field ambiguity surface using winter profile for the midpoint robust matched-field processor in the presence of a −1 m/s sound-speed uncertainty in the water column, source at 40 m depth and 22 km range; robust design over uncertainty neighborhood (0.0, −0.8).*

there is uncertainty.

Figure 6 illustrates the range/depth surface when the robust minimax(0.0,−0.8) processor is applied with the maximum uncertainty condition, i.e., −1 m/s perturbation of the surface sound speed. Figure 6 illustrates the performance obtained using the midpoint processor for a source is at a depth of 40 m and range of 22 km. Comparing this figure with Fig. 4b it can be seen that the midpoint robust processor provides a significant improvement. When the midpoint processor is used the source peak is located at the correct source location and the sidelobes are significantly reduced. This example clearly illustrates that robust matched-field methods can significantly improve localization performance in a realistic shallow-water situation in the presence of uncertainty about the sound speed profile.

Figure 7 provides an indication of the performance of the robust midpoint (0.0,−0.8) processor as a function of source range. Figure 7a illustrates the peak-to-sidelobe ratio for the nominal processor and the midpoint processor for a source at 40 m depth and 12 km range. At this relatively close range it is seen that the impact of the sound-speed uncertainty is not serious and that the nominal processor performs better than the midpoint processor over the range of sound-speed uncertainty. Figure 7b illustrates the same situation for a source at 40 m depth and 16 km range. In this case the robust midpoint processor outperforms the nominal processor for all sound-speed uncertainties greater than about −0.2 m/s. Similarly, Figures 7c,d illustrate the situation for a source at 40 m depth and ranges of 20 km and 24 km respectively. At these ranges the robust processor maintains a significantly larger peak-to-sidelobe ratio over most of the sound-speed uncertainty.

Figure 8 provides a comparison of the peak-to-sidelobe ratio for the three robust methods using the winter profile with sound-speed uncertainty. The peak-to-sidelobe ratio for the nominal processor is also illustrated for comparison. The design neigh-

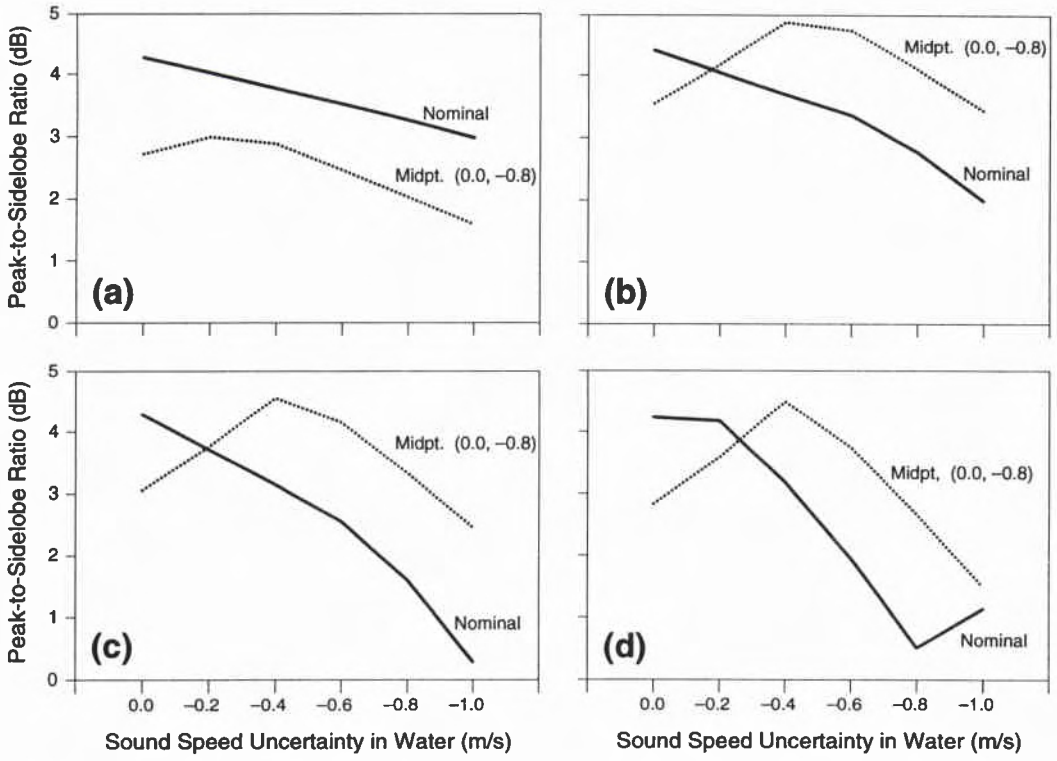

Figure 7 *Peak-to-sidelobe ratio as a function of sound-speed uncertainty in the water column for the 'midpoint' robust processor using the winter profile. Results are shown for the midpoint processor designed over uncertainty neighborhood (0.0, −0.8) and the nominal processor for a source at 40 m depth and range (a) 12 km, (b) 16 km, (c) 20 km, and (d) 24 km.*

borhood is the same for all three processors, (0.0,−0.8). This figure illustrates the performance for a source at a depth of 40 m and a range of 22 km. It is seen that all three robust processors provide a significant improvement with respect to that of the nominal processor. The performance of the minimax and midpoint processors is almost identical, whereas the performance of the mean processor is somewhat degraded with respect to the other two.

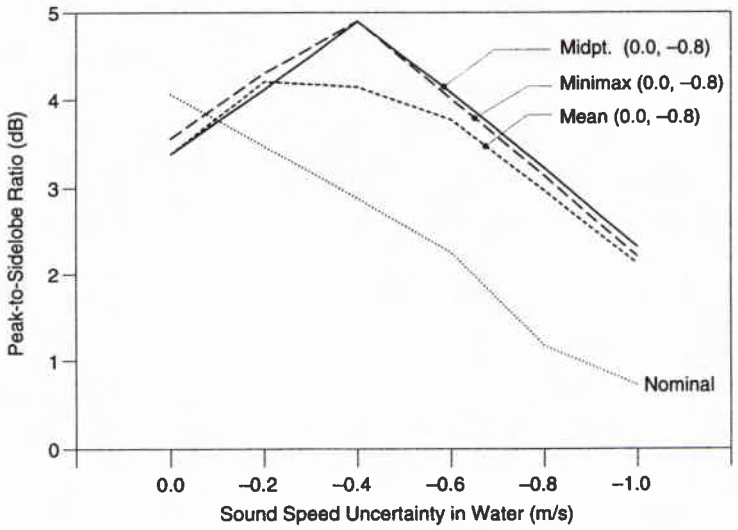

Figure 8 *Peak-to-sidelobe ratio as a function of sound-speed uncertainty in the water column for the minimax, midpoint and mean robust processors using the winter profile. Results are shown for the robust processors designed over uncertainty neighborhood (0.0, −0.8) and the nominal processor for a source at 40 m depth and 22 km range.*

4.2. SOUND-SPEED UNCERTAINTY IN THE WATER COLUMN: SUMMER PROFILE

In this subsection we present the performance obtained using the robust and nominal matched-field processors in the presence of sound-speed uncertainty with the canonical summer environment. For the summer case the sound-speed uncertainty was generated by perturbing the isovelocity layer from the nominal value of 1520 m/s to 1519 m/s in steps of 0.2 m/s. The remainder of the profile below the isovelocity layer was left unperturbed. This uncertainty in sound speed is less severe than that introduced into the winter profile but it is partially representative of the surface warming/cooling effect expected in the summer.

Figures 9a,b illustrate the matched-field range/depth ambiguity surfaces for the perfect knowledge case and for the −1 m/s uncertainty case, respectively, for a source at a depth of 40 m and at a range of 22 km. Examining Fig. 9a it is seen that the maximum sidelobes are on the order of 4 dB down from the source peak and that the source peak is well defined and at the correct location. In comparison, examining Fig. 9b the impact of the sound-speed uncertainty is easily observed. The sidelobe structure has changed significantly, there are many sidelobes within 5 dB of the peak and the highest sidelobe has a peak-to-sidelobe ratio of only 0.5 dB.

Figure 10 illustrates performance, peak-to-sidelobe ratio, for the robust midpoint processor for various design neighborhoods and the nominal processor. Comparing Figs. 10 and 5, it is seen in contrast to the winter profile case there is no one single

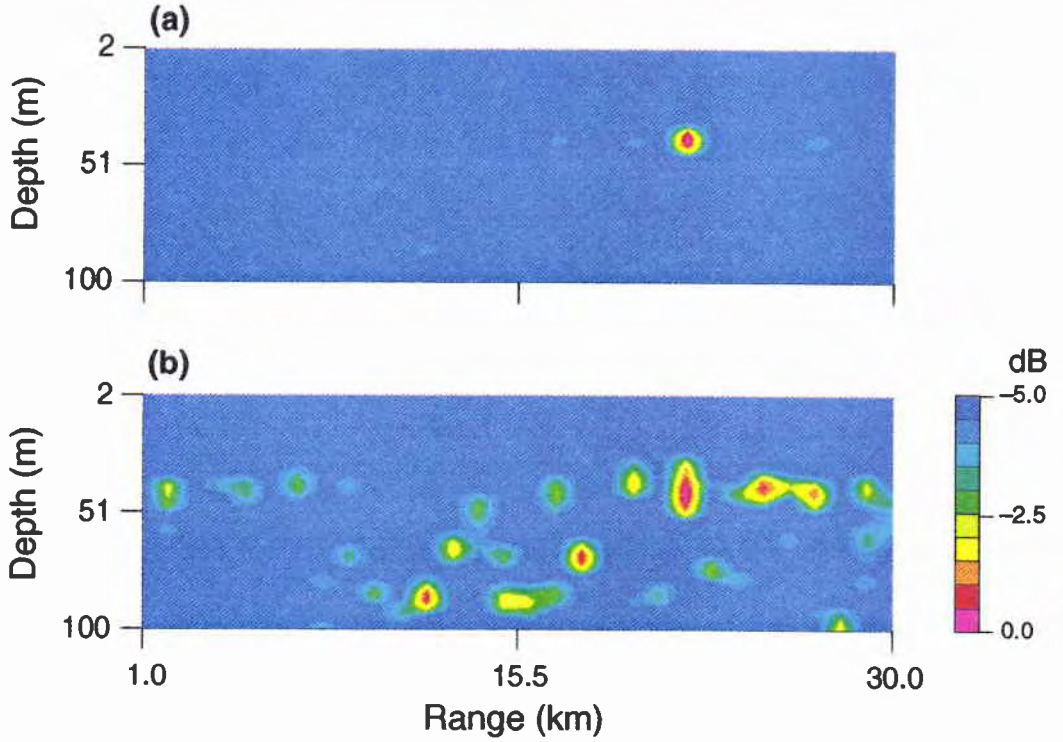

Figure 9 *Matched-field ambiguity surfaces using summer profile for a source at 40 m depth and 22 km range, (a) nominal environment with no uncertainty, (b) with −1 m/s sound-speed uncertainty in the water column.*

design neighborhood that performs well over the full range of uncertainty. For example, midpoint (0.0,−0.4) provides gains with respect to the nominal for small uncertainty, i.e., −0.2 to −0.4 m/s. At large uncertainty, −1 m/s, the peak-to-sidelobe ratio is almost the same as the nominal processor. The midpoint (0.0,−0.6) processor appears to provide the most gain across the uncertainty range, although it performs poorly for the perfect knowledge case. Over the entire range of sound-speed uncertainty the midpoint (0.0,−0.6) processor provides a range/depth ambiguity surface with the peak at the correct source location.

Figure 11 illustrates the range/depth surface for the midpoint (0.0,−0.6) processor under the maximum uncertainty condition, −1 m/s perturbation of the surface sound speed, for a source at a depth of 40 m and a range of 22 km. Comparing this figure with Fig. 9b, it is noted that there are fewer sidelobes and that the amplitudes of the sidelobes are reduced. The peak-to-sidelobe ratio has increased from 0.5 dB to 1.38 dB, again demonstrating a performance gain for the robust processor with respect to the nominal processor in an uncertain environment.

Figure 12 illustrates peak-to-sidelobe performance as a function of sound-speed uncertainty for a source at a depth of 40 m and a range of 22 km. It is seen that all three robust processors provide a significant improvement with respect to the

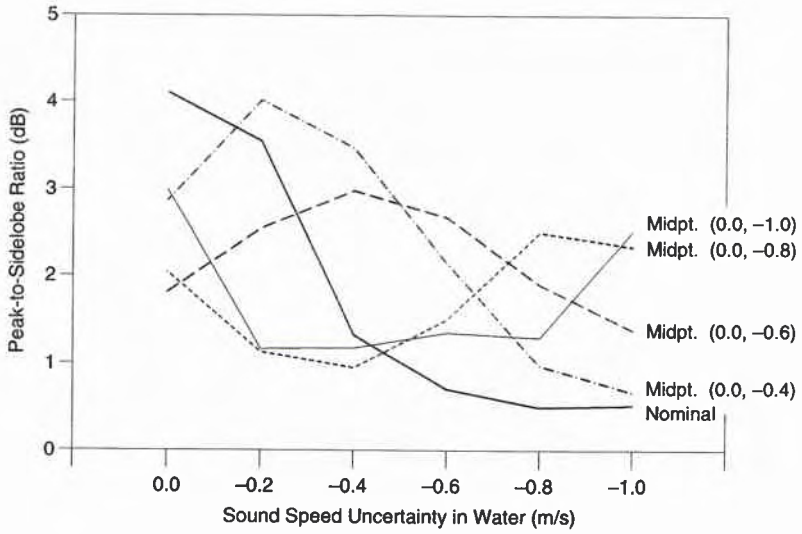

Figure 10 *Peak-to-sidelobe ratio as a function of sound-speed uncertainty in the water column for the 'midpoint' robust processor using the summer profile. Results are shown for the midpoint processor designed using four different uncertainty neighborhoods and for the nominal processor for a source at 40 m depth and 22 km range.*

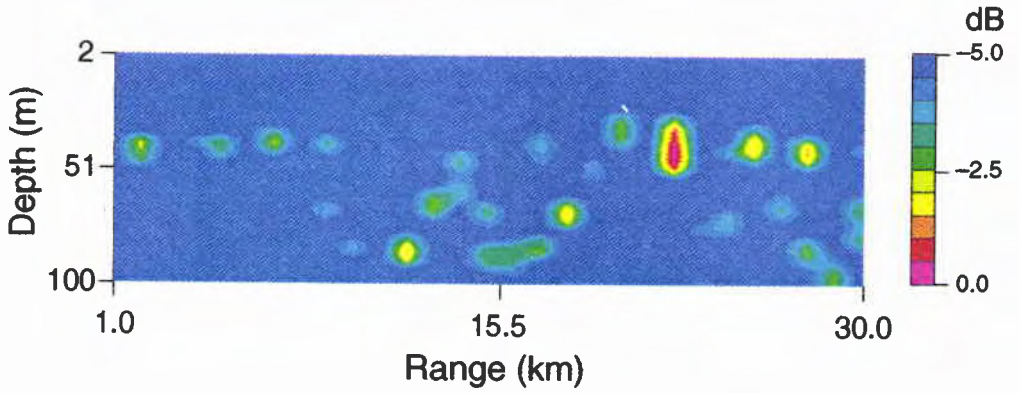

Figure 11 *Matched-field ambiguity surface using summer profile for the midpoint robust matched-field processor in the presence of a −1 m/s sound-speed uncertainty in the water column, source at 40 m depth and 22 km range; robust design over uncertainty neighborhood (0.0, −0.6).*

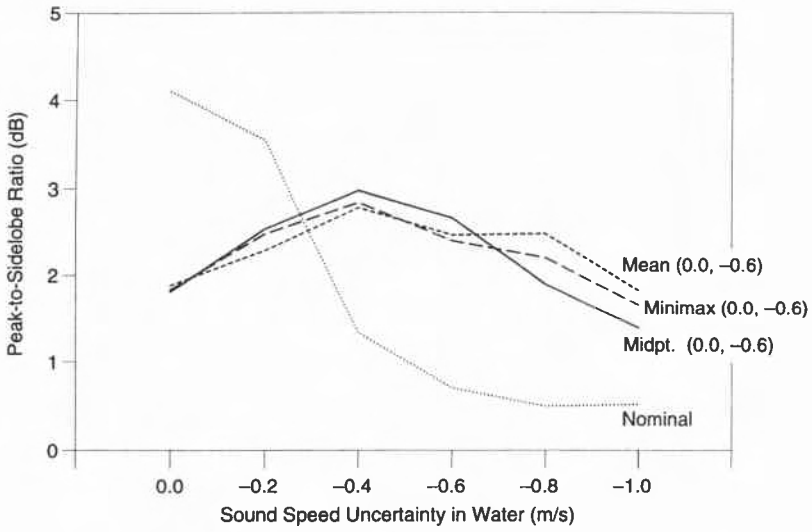

Figure 12 *Peak-to-sidelobe ratio as a function of sound-speed uncertainty in the water column for the minimax, midpoint and mean robust processors using the summer profile. Results are shown for the robust processors designed over uncertainty neighborhood (0.0, −0.6) and for the nominal processor for a source at 40 m depth and 22 km range.*

nominal processor and that the performance of the minimax, midpoint and mean processors is similar.

4.3. CHANNEL DEPTH UNCERTAINTY: WINTER PROFILE

In this subsection we examine the performance results obtained in the presence of channel depth uncertainty for the canonical winter profile. The nominal channel depth was 120 m, the uncertainty was generated by perturbing the depth from 120 m to 121 m in steps of 0.2 m. It was shown in Ref. [11] that a depth uncertainty of 1 m may seriously degrade the performance of matched-field processors.

Figures 13 a,b illustrate the matched-field range/depth ambiguity surfaces for the perfect knowledge case and for the +1 m depth uncertainty case, respectively, for a source at a depth of 40 m and at a range of 12 km. It is seen from Fig. 13b that, even at the relatively close range of 12 km, the 1 m perturbation of depth seriously degrades the performance of the process. The largest peak on the surface is not at the correct source location and there are many sidelobes within 1 dB of the largest peak. The peak-to-sidelobe ratio is only 0.7 dB.

Figure 14 illustrates an overview of performance, peak-to-sidelobe ratio, for both the nominal and robust processors as a function of channel depth uncertainty. It is seen that the peak-to-sidelobe ratio for the nominal processor decreases rapidly from 4.2 dB to almost zero as the uncertainty varies from 0.0 to 0.6 m. The other curves

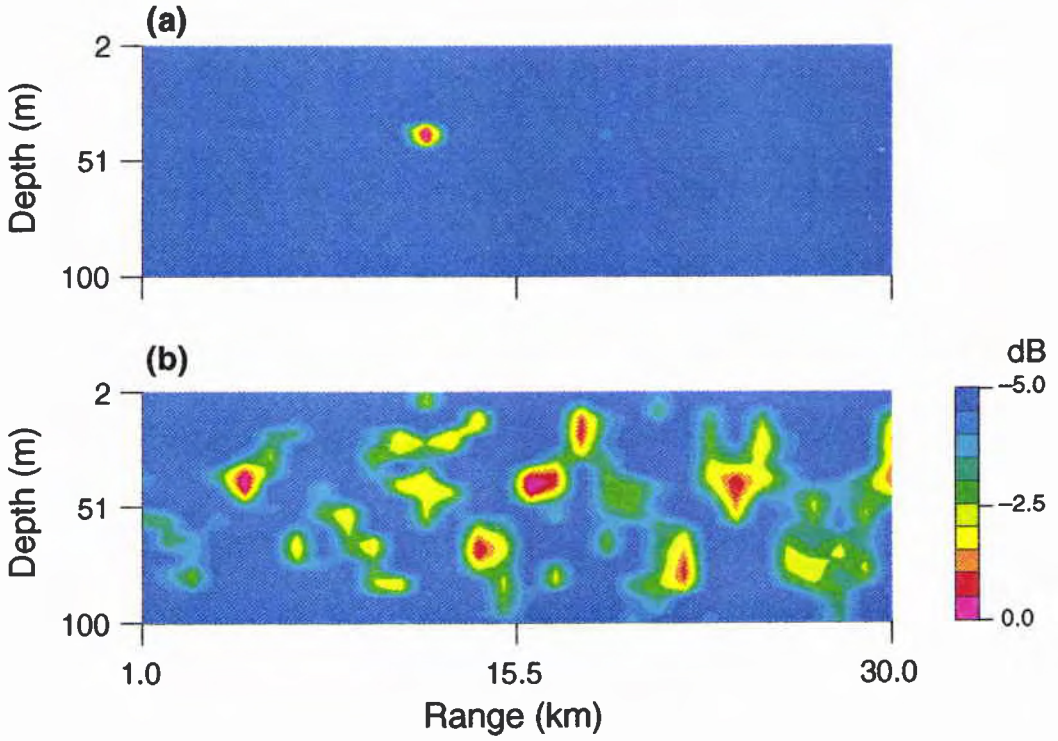

Figure 13 *Matched-field ambiguity surfaces using winter profile for a source at 40 m depth and 12 km range, (a) nominal environment with no uncertainty, (b) with a 1 m channel depth uncertainty.*

illustrate the performance of the midpoint processor for various design neighborhoods. Each of the designs provides a gain with respect to the nominal processor, but there is no single design that yields improved performance across the entire range of depth uncertainty. The design midpoint (0.4,0.8) provides a performance improvement over a fairly large range of depth uncertainty. For small uncertainty, less than 0.3 m, the nominal processor performs well, for uncertainty greater than 0.3 m the performance of the nominal processor degrades rapidly whereas the midpoint (0.4,0.8) processor performs quite well, even for a 1 m depth uncertainty. Over the range of depth uncertainty from 0 to 1 m the midpoint (0.4,0.8) processor provides a range/depth ambiguity surface with the peak at the correct source location for all cases except for the certain case.

Figure 15 illustrates the range/depth surface for the midpoint (0.4,0.8) robust processor for a source at 40 m and at 12 km under a 1 m depth uncertainty. Comparing this surface with that of Fig. 13b it is seen that the performance is improved significantly. With the midpoint (0.4,0.8) processor the largest peak in now at the correct source location and the peak-to-sidelobe ratio has increased to almost 2 dB.

Figure 16 illustrates a comparison of the three robust methods and the nominal processor for the winter profile with channel depth uncertainty. The source was

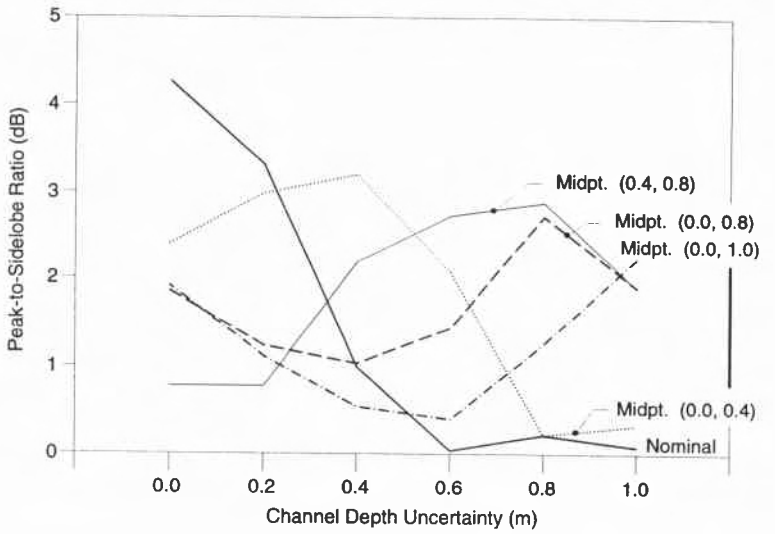

Figure 14 *Peak-to-sidelobe ratio as a function of channel depth uncertainty for the 'midpoint' robust processor using the winter profile. Results are shown for the midpoint processor designed using four different uncertainty neighborhoods and for the nominal processor for a source at 40 m depth and 12 km range.*

located at 40 m depth and at 12 km range. It is seen that all three robust processors perform significantly better than the nominal processor for a depth uncertainty greater than about 0.3 m. Peak-to-sidelobe ratios on the order of 2 to 3 dB are observed over the entire range of uncertainty greater than 0.3 m. The performance of the three robust processors minimax, midpoint, and mean is largely the same over the range of uncertainty.

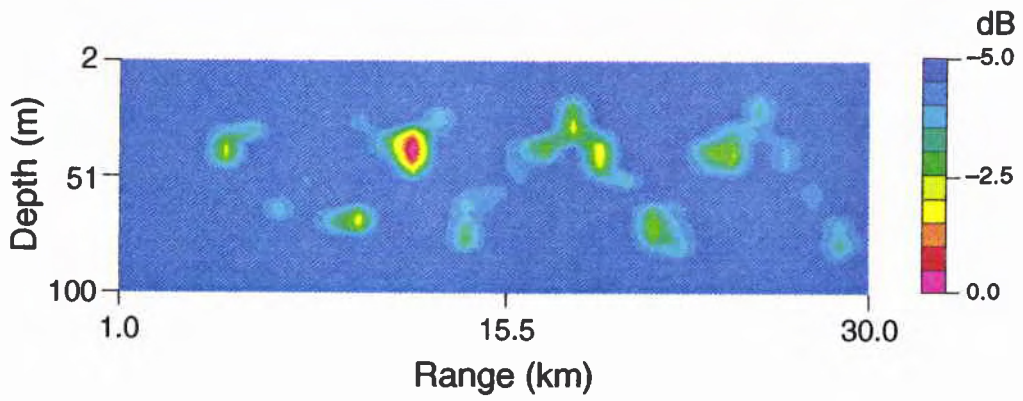

Figure 15 *Matched-field ambiguity surface using winter profile for the midpoint robust matched-field processor in the presence of a 1 m channel depth uncertainty, source at 40 m depth and 12 km range; robust design over uncertainty neighborhood (0.4, 0.8).*

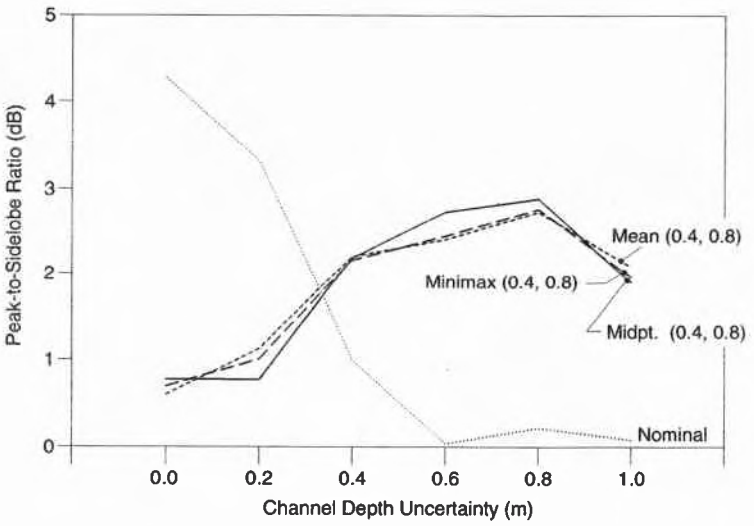

Figure 16 *Peak-to-sidelobe ratio as a function of channel depth uncertainty for the minimax, midpoint and mean robust processors using the winter profile. Results are shown for the robust processors designed over uncertainty neighborhood (0.4, 0.8) and for the nominal processor for a source at 40 m depth and 12 km range.*

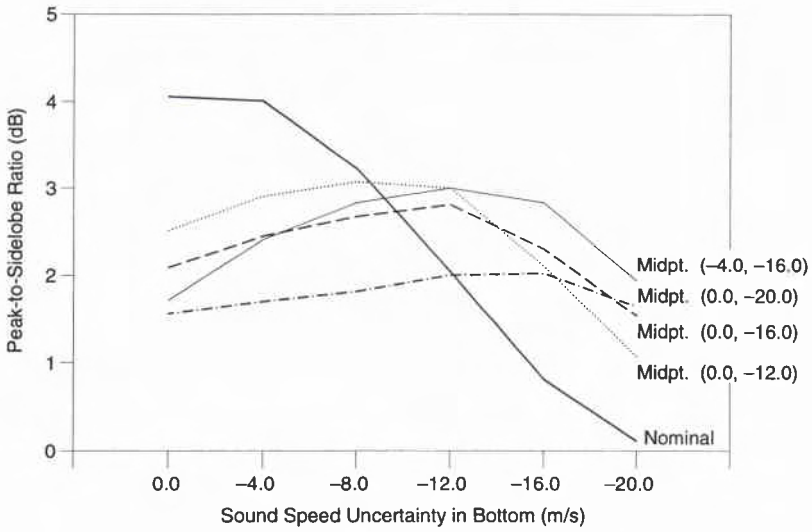

Figure 17 *Peak-to-sidelobe ratio as a function of sound-speed uncertainty in the bottom for the 'midpoint' robust processor using the winter profile. Results are shown for the midpoint processor designed using four different uncertainty neighborhoods and for the nominal processor for a source at 40 m depth and 22 km range.*

4.4. SOUND-SPEED UNCERTAINTY IN THE BOTTOM: WINTER PROFILE

Figure 17 illustrates an overview of performance, peak-to-sidelobe ratio, for both the nominal and robust processors as a function of bottom sound-speed uncertainty. It is seen that the peak-to-sidelobe ratio for the nominal processor decreases almost monotonically from 4 dB to almost zero as the uncertainty varies from 0.0 to −20.0 m/s. The other curves illustrate the performance of the midpoint processor for various design neighborhoods. Each of the designs provides a gain with respect to the nominal processor for uncertainty greater than about −8.0 m/s. There is no single design which yields improved performance across the entire range of depth uncertainty. The design, midpoint (0.0,−16.0), provides a performance improvement over a fairly large range of uncertainty. For small uncertainty, less than −8.0 m/s, the nominal processor performs well, for uncertainty greater than −8.0 m/s the performance of the nominal processor degrades rapidly whereas the midpoint processors perform quite well, even for a −20 m/s sound-speed uncertainty. With an uncertainty of −20 m/s the nominal processor provides a peak-to-sidelobe ratio of only 0.1 dB, whereas the midpoint processor provides a ratio of about 1.5 dB. Over the entire range of sound-speed uncertainty the midpoint (0.0,−16.0) processor provides a range/depth ambiguity surface with the peak at the correct source location.

Figure 18 illustrates a comparison of the three robust methods and the nominal processor for the winter profile with bottom sound-speed uncertainty. The source was located at 40 m depth and at 22 km range. It is seen that all three robust processors perform significantly better than the nominal processor for sound-speed uncertainty greater than about −8.0 m/s. All three robust processors are based on

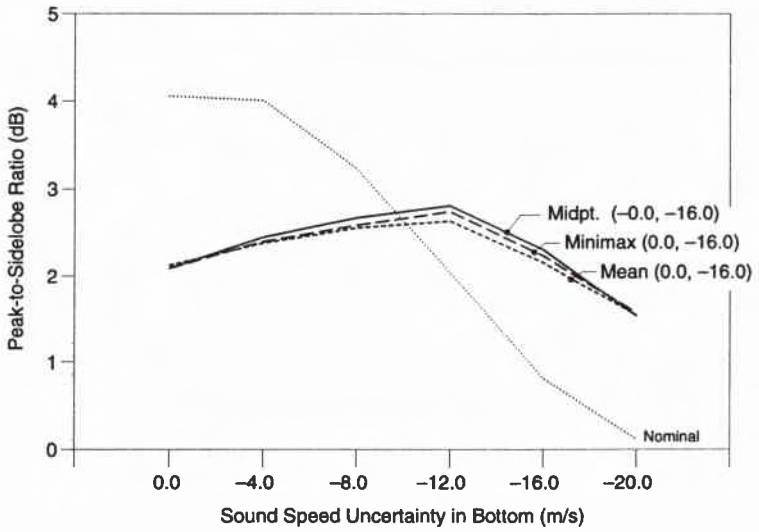

Figure 18 *Peak-to-sidelobe ratio as a function of sound-speed uncertainty in the bottom for the minimax, midpoint and mean robust processors using the winter profile. Results are shown for the robust processors designed over uncertainty neighborhood (0.0, −16.0) and for the nominal processor for a source at 40 m depth and 22 km range.*

a design neighborhood of (0.0,−16.0). Peak-to-sidelobe ratios on the order of 1.5 to 3 dB are observed over the entire range of uncertainty. The performance of the three robust processors minimax, midpoint, and mean is largely the same over the range of uncertainty.

5 Discussion

Robust methods for matched-field processing which take into account *a priori* knowledge about environmental uncertainty have been developed, see Ref. [13]. In this report the performance of these robust matched-field methods has been evaluated and compared to that of the conventional non-robust method in terms of the peak-to-sidelobe ratio as a function of environmental parameter uncertainty.

A variety of environmental uncertainty types were considered in the context of a shallow water example. Uncertainty in the sound speed profile for both a winter and summer profile, uncertainty in the channel depth for a winter profile and uncertainty in the speed of sound in the bottom for a winter profile were all considered. In addition the performance as a function of the source location in the water column was also considered. In all of the cases the robust methods outperformed the nominal processor when the environmental knowledge was uncertain. The performance of the robust methods was shown, as expected, to depend on the specification of the design neighborhood. Also, as expected, the nominal processor always performed better than the robust processor when there was no uncertainty about the environmental knowledge.

As with all matched-field processing problems it is impossible it provide performance results over the entire space of system and environmental parameters. In this report the system parameters were held fixed and the performance was evaluated over a reasonably wide range of environmental parameters. The results presented herein clearly indicate that the robust methods of Ref. [13] provide improved matched-field processing performance when environmental knowledge is uncertain.

The assumption that the environment is range-independent was made for convenience. Since the design of the robust processor, of Section 3, is based on simple bounds for the environmental parameter uncertainty, the application of these robust methods to a range-dependent environment should follow directly. Simulations in a range-dependent environment with random environmental parameter uncertainty should be carried out to verify that the performance gains for this case are similar to that of the range-independent case.

It should be noted that the implementation of these robust methods is quite straightforward. It should also be noted that these methods do not require a significantly larger computational load than that of conventional methods.

In general these methods require about a factor of two increase in computation time with respect to conventional non-robust methods.

Document Data Sheet

NATO UNCLASSIFIED

Report no. changed (Mar 2006): SR-215-UU

Security Classification		Project No.
NATO UNCLASSIFIED		02
Document Serial No.	**Date of Issue**	**Total Pages**
SR-215	November 1993	35 pp.

Author(s)

D.F. Gingras

Title

Robust broadband matched-field processing:
Performance in shallow water by simulation

Abstract

An issue of concern for matched-field processing is the strong dependence between performance and precise knowledge about the environmental parameters. Recently a robust matched-field processor based on minimax robust filtering methods was developed. In this report simulation methods are employed to evaluate the performance of the minimax robust method as well as other robust methods for a range-independent shallow-water environment. The performance of the robust methods is compared with that of the nominal processor, that is, the processor based on a single set of environmental parameters thought to be closest to the actual. The matched-field processing performance is evaluated in terms of the peak-to-sidelobe ratio, the simulation results indicate that the robust methods provide significant performance improvements over the nominal processor in the presence of uncertainty in water-column sound-speed, channel depth and sound speed in the bottom.

Keywords

Matched-field processing, minimax methods, normal-mode modelling.

Issuing Organization

North Atlantic Treaty Organization
SACLANT Undersea Research Centre
Viale San Bartolomeo 400, 19138 La Spezia, Italy

tel: 0187 540 111
fax: 0187 524 600
telex: 271148 SACENT I

*[From N. America: SACLANTCEN CMR-426
(New York) APO AE 09613]*

NATO UNCLASSIFIED

Report no. changed (Mar 2006): SR-215-UU

Initial Distribution for SR-215

Ministries of Defence	
JSPHQ Belgium	2
DND Canada	10
CHOD Denmark	8
MOD France	8
MOD Germany	15
MOD Greece	11
MOD Italy	10
MOD Netherlands	12
CHOD Norway	10
MOD Portugal	5
MOD Spain	2
MOD Turkey	5
MOD UK	20
SECDEF US	54
NATO Authorities	
NAMILCOM	2
SACLANT	3
CINCIBERLANT	1
COMSUBACLANT	1
SCNR for SACLANTCEN	
SCNR Belgium	1
SCNR Canada	1
SCNR Denmark	1
SCNR Germany	1
SCNR Greece	1
SCNR Italy	1
SCNR Netherlands	1
SCNR Norway	1
SCNR Portugal	1
SCNR Spain	1
SCNR Turkey	1
SCNR UK	1
SCNR US	2
French Delegate	1
SECGEN Rep. SCNR	1
NAMILCOM Rep. SCNR	1
National Liaison Officers	
NLO Belgium	1
NLO Canada	1
NLO Denmark	1
NLO Germany	1
NLO Italy	1
NLO Netherlands	1
NLO UK	1
NLO US	1
Total external distribution	204
SACLANTCEN Library	21
Total number of copies	225